Difference in Topographic Pattern of Prelaminar and Neuroretinal Rim Thinning Between Nonarteritic Anterior Ischemic Optic Neuropathy and Glaucoma

Eun Jung Lee, Jong Chul Han, Do Young Park, and Changwon Kee

Department of Ophthalmology, Samsung Medical Center, Sungkyunkwan University School of Medicine, Seoul, Korea

Correspondence: Changwon Kee, Department of Ophthalmology, Samsung Medical Center, Sungkyunkwan University School of Medicine, 81 Irwon-ro, Gangnam-gu, Seoul 06351, Korea;
ckee@skku.edu.

Submitted: February 16, 2019
Accepted: May 7, 2019

Citation: Lee EJ, Han JC, Park DY, Kee C. Difference in topographic pattern of prelaminar and neuroretinal rim thinning between nonarteritic anterior ischemic optic neuropathy and glaucoma. *Invest Ophthalmol Vis Sci*. 2019;60:2461–2467. https://doi.org/10.1167/iovs.19-26891

Purpose. To compare the local distribution of prelaminar and neuroretinal rim (NRR) thickness between eyes with nonarteritic anterior ischemic optic neuropathy (NAION) and normal tension glaucoma (NTG) using enhanced depth imaging spectral-domain optical coherence tomography (OCT).

Methods. This cross-sectional study included pairs of NAION and NTG patients, and controls. We measured the central prelaminar thickness; Bruch's membrane opening (BMO)—horizontal (HRW), minimal (MRW), and vertical rim widths (VRW), and vertical/horizontal thicknesses at knee of curve at rising curvature of the cup wall. HV ratio was calculated as BMO-HRW/BMO-VRW. The six thicknesses and their differences were compared.

Results. We had 12 pairs, with comparable visual field loss and retinal nerve fiber layer (RNFL) thickness between NAION and NTG. Within the optic nerve head (ONH), BMO-MRW, BMO-HRW, horizontal width at the knee of curve, and central prelaminar tissue showed significantly larger values in NAION compared to NTG ($P < 0.05$). The difference of NRR thickness between NAION and NTG increased in a centripetal manner, being maximum at the knee of curve. The mean HV ratio was 1.63 in NAION, 0.83 in NTG, and 1.06 in controls ($P < 0.001$). OCT showed disproportionately less altered prelaminar tissue in NAION.

Conclusions. NAION and NTG showed significantly different distributions of prelaminar and NRR tissue thicknesses despite similar RNFL thicknesses, with the maximal difference being the horizontal cup wall thickness at the knee of curve. Sparing of prelaminar tissue loss characterized the ONH in NAION. OCT might aid in differential diagnosis based on local variation in thinning patterns.

Keywords: glaucoma, nonarteritic anterior ischemic optic neuropathy, optical coherence tomography, prelaminar tissue, neuroretinal rim

Optic disc cupping is an important indicator of glaucomatous change.[1] While vertical cupping and obliteration of the neuroretinal rim (NRR) are highly useful signs of glaucoma,[2] optic disc pallor is characteristic of non-glaucomatous optic neuropathies such as ischemic optic neuropathy, compressive optic neuropathy, and traumatic optic neuropathy.[3,4]

Although it had been previously believed that disc cupping was absent in optic disc pallor, several investigations have demonstrated significant decrease of NRR in ischemic optic neuropathies with disc pallor. Contour evaluation by scanning laser ophthalmoscopy successfully demonstrated a small but significant increase in the cup size compared to unaffected fellow eyes,[5] as well as greater cupping in glaucoma than in ischemic optic neuropathy.[6] Most recently, optical coherence tomography (OCT) enabled a quantitative comparison of the NRR between glaucoma and nonarteritic ischemic optic neuropathy (NAION) through a direct measurement of the thickness of the retinal nerve fiber layer (RNFL).[7,8] Fard et al.[7] evaluated deep optic nerve head (ONH) structures including the lamina cribrosa (LC) and demonstrated greater LC depth and thinner prelaminar tissue in glaucoma than in NAION eyes. Furthermore, Resch et al.[8] evaluated ONH parameters including Bruch's membrane opening (BMO)-based minimum rim width (MRW), and showed that NAION eyes had parameters similar to those seen in healthy controls under similar RNFL thickness compared to glaucoma eyes. The results revealed the significance of OCT in distinguishing glaucoma from NAION.[8]

It is not known whether prelaminar and NRR thinning in ischemic optic neuropathies have a morphologic similarity to that of glaucoma at various points of prelaminar tissue or largely based on tissue thinning at specific locations. There is a possibility that the distribution profile of prelaminar tissue thickness change would be specific to the underlying disease. In other words, the disease diagnosis might determine the specific points where the significant tissue thinning would occur in a selective manner. Due to the obvious difference in NRR morphology between the NAION and glaucoma eyes, measurement of NRR thickness may be required in more than one direction to show at which location the difference becomes most notable.

Therefore, we investigated the profiles of prelaminar tissue thickness in NAION and glaucoma at the following locations; above the LC center in vertical direction, at the location where the cup wall began to rise in horizontal and vertical directions, and in horizontal, vertical, and minimal widths at the BMO margin. We aimed to delineate the difference in the distribution

pattern of prelaminar tissue thickness between optic disc pallor and glaucomatous cupping, in order to achieve a differential anatomic understanding of local NRR contour.

Methods

This retrospective, cross-sectional study included patients with NAION, normal tension glaucoma (NTG), and healthy controls. The research protocol was approved by the Institutional Review Board at Samsung Medical Center and all research was performed in accordance with the tenets of the Declaration of Helsinki.

Patient Inclusion and Examination

We performed comprehensive ophthalmic examinations, including measurement of visual acuity and refraction, IOP measurement with Goldmann applanation tonometry, slit-lamp biomicroscopy, gonioscopic examination, dilated stereoscopic examination of the optic nerve head, color and red-free fundus photography, Humphrey Swedish Interactive Threshold Algorithm visual field tests using the central 30-2 Humphrey Field Analyzer (HFA model 640 or model 740; Humphrey Instruments Inc., San Leandro, CA, USA), ultrasound pachymetry (Tomey SP-3000; Tomey Ltd., Nagoya, Japan), high-definition OCT (Cirrus; Carl Zeiss Meditec, Dublin, CA, USA), and enhanced depth imaging (Spectralis OCT; Heidelberg Engineering, Heidelberg, Germany).

NAION was diagnosed based on characteristic clinical findings, such as swollen disc, segmental optic atrophy, altitudinal visual field (VF) defect, or disc pallor. Patients were followed-up without magnetic resonance imaging (MRI) examination only when all their clinical findings were compatible with those of NAION (i.e., altitudinal-pattern VF defects with corresponding RNFL loss or disc pallor). When any sign suggestive of secondary optic atrophy due to an intracranial lesion was noted, an MRI examination was performed, and the patient was excluded from the study. The presence of optic disc pallor was judged by two independent investigators and had to be corresponding to RNFL defect and the VF test. Unilateral patients were included, and the affected eye was utilized for analysis.

Diagnosis of NTG was based on the presence of an NRR or RNFL defect, visible on slit-lamp biomicroscopy, color photographs, and red-free fundus photographs, as well as a consistent glaucomatous pattern in two consecutive VF tests, with pattern standard deviation outside the normal limits ($P < 0.05$). We selected NTG to exclude the effect of high IOP on OCT images. The normal control group consisted of healthy eyes without any evidence of VF or RNFL defects, IOP elevation, or disc hemorrhage.

We excluded the patients with the following conditions that could have affected the NRR parameters: tilted discs with an ovality index >1.1; untreated IOP >21 mm Hg; optic disc pallor from concomitant retinal diseases, such as diabetic retinopathy, retinal venous obstruction, retinal arterial obstruction, or retinitis pigmentosa; and previous unilateral cataract surgery to exclude pseudophakic pallor. Ovality index of the optic disc was defined as the ratio of the longest and shortest disc diameters by the clinical optic disc margin on color photographs using ImageJ (http://imagej.nih.gov/ij/; provided in the public domain by the National Institutes of Health, Bethesda, MD, USA).

We matched the patients by disc area measured using the en face infrared OCT images with the inbuilt OCT software (Heidelberg Eye Explorer, version 6.8a; Heidelberg Engineering), with the difference between matched eyes to be within 0.1 mm^2. Between the NTG and control groups, only one eye of a patient was matched, and for the NTG eyes, degree of VF defect and RNFL thickness were also matched to NAION eyes.

Evaluation of Local Prelaminar and NRR Tissue Thicknesses

Enhanced depth imaging (EDI) OCT scans were obtained using 24 radial-line B-scans, each at an angle of 7.5° and centered on the optic disc. The scaling of the OCT scanner was adjusted to 1:1 μm before measurement. All measurements were performed amid the degenerated RNFL, where the characteristic NRR changes were most distinct in each group. After a thorough review of consecutive cuts in radial images, the centermost location of sectoral pallor and the thinnest NRR location were chosen in NAION and NTG, respectively. Measurements in controls were performed in the same mirror direction. Only when overlying large vessels prevented interpretation of the structures, the next image was used, so the thickness of vessels would not be included into the measurement.

Prelaminar tissue thickness was measured as the vertical distance between the anterior surface of the lamina cribrosa and the vitreal interface. The anterior surface of the LC was defined as the location where high reflectivity started beneath the optic disc cup on OCT.[9]

We measured six prelaminar and NRR tissue thicknesses (Fig. 1). Three measurements at the NRR, the BMO-horizontal rim width (HRW), BMO-MRW, and BMO-vertical rim width (VRW), and central prelaminar tissue thickness in a vertical direction above the LC center were measured. We allocated a point corresponding to the knee of curve that is a point where the curvature has a local maximum around the beginning of the cup wall (Fig. 1B), where the measurement of thickness in horizontal direction would approximately reflect the maximum thickness of cup wall. We calculated a new variable, horizontal-to-vertical (HV) ratio, as follows: BMO-HRW/BMO-VRW.

In addition, the RNFL thicknesses in global and affected sectors of OCT measurement were obtained from Cirrus HD-OCT measurements.

Statistical Analysis

To evaluate the interobserver reproducibility of knee of curve allocation, two independent observers (EJL, DYP) separately selected knee of curve point and measured horizontal and vertical rim widths at that point. The absolute agreement of the two observers' measurements was calculated with the intraclass correlation coefficient (ICC) from a 2-way mixed effect model. Intraobserver reproducibility was also calculated by repeated measurements made by EJL.

For a matched comparison between the NAION (group A), NTG (group B), and control (group C) groups, we performed Friedman's test and Wilcoxon signed-rank test. P value was adjusted for multiple comparison with Bonferroni correction. Demographic characteristics and clinical characteristics, such as IOP, VF index, and refractive error, as well as prelaminar tissue thickness measurements and calculated ratio, were compared. Power for Wilcoxon signed-rank test between NAION and glaucoma was calculated to evaluate the adequateness of the sample size in the study based on the given average and standard deviation values of the difference of BMO-HRW between NAION and glaucoma, with type I error probability of 0.05 for two-sided test. Statistical analyses were performed using statistical software (SPSS version 23.0; SPSS, Inc., Chicago, IL, USA) and G*Power version 3.1.[10] A value of $P < 0.05$ was considered statistically significant.

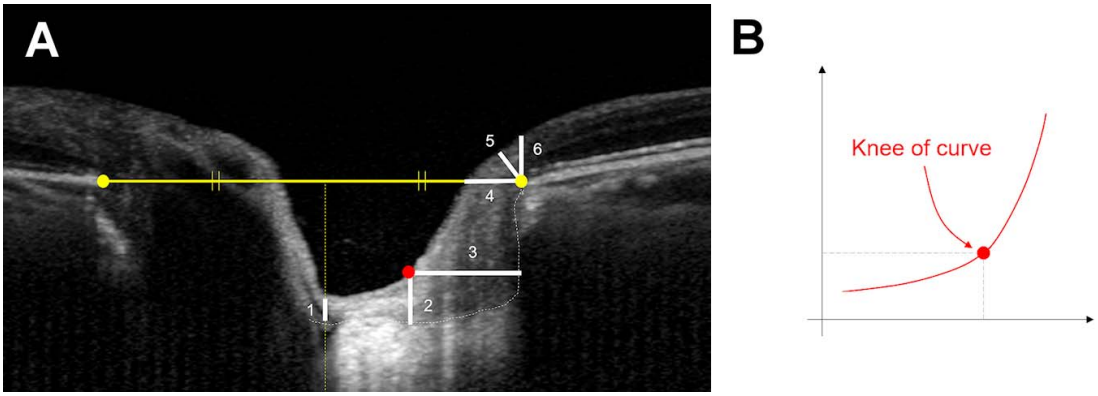

FIGURE 1. (**A**) Measurement of prelaminar thicknesses including the neuroretinal rim structures. (*1*) Prelaminar tissue thickness measured in vertical direction above the LC center. (*2*) Prelaminar tissue thickness at the knee of curve (*red dot*) in a vertical direction. (*3*) Prelaminar tissue thickness at the knee of curve (*red dot*) in a horizontal direction. (*4*) BMO-horizontal rim width. (*5*) BMO-minimum rim width. (*6*) BMO-vertical rim width. The knee of curve shows a point where the curvature has a local maximum around the beginning of the cup wall. All measurement axes were based on the BMO plane. (**B**) A schematic illustration for knee of curve point designation.

RESULTS

Clinical Characteristics of the Patients

We enrolled 12 pairs of patients. Three eyes with NAION were excluded with acute swelling throughout the optic nerve due to the possibility of optic neuritis. All eyes were in chronic stage and no evidence of swelling or acute episode within 6 months was observed. The numbers of recruited patients were sufficient to show significant differences between BMO-HRW and BMO-MRW, with calculated power of 99.97% and 88.9%, respectively.

The demographic features and degree of RNFL or VF loss were comparable between NAION and NTG groups (Table 1). In the NAION group, the most common involvement of RNFL loss was in the superotemporal direction (11, 91.7%) with corresponding inferior VF defect.

Distribution of Local Prelaminar and NRR Tissue Thicknesses

Horizontal rim width measurement at the knee of curve showed excellent intra-observer (ICC = 0.992 and 95% confidence interval [CI] = 0.984–0.996) and interobserver (ICC = 0.956 and 95% CI = 0.913–0.977) reproducibility (all $P < 0.001$). Vertical rim width measurement at the knee of curve also showed excellent intra-observer (ICC = 0.992 and 95% CI = 0.985–0.996) and interobserver (ICC = 0.957 and 95% CI = 0.915–0.978) reproducibility (all $P < 0.001$).

Under highly similar disc area and BMO width, all thickness parameters were significantly greater in NAION than in NTG, except for vertical knee of curve thickness and BMO-VRW (Table 2). The degree of difference varied depending on the location of the measurement. The difference was maximal at the knee of curve, measured with the horizontal width, and decreased thereafter in the order of BMO-HRW, BMO-MRW, and BMO-VRW, where the difference became insignificant.

At the outermost measurement location of the ONH, BMO-VRW revealed that both NAION and NTG showed significantly decreased thickness, without any difference between them. Within-ONH location starting from BMO-MRW, the relative magnitudes of thickness values were in decreasing order of control, NAION, and NTG, in line with previous studies. The six measured thicknesses in NAION, NTG, and control eyes are shown in Figure 2A. The distribution showed marked variation by measurement locations, and the difference in thickness between NAION and NTG was maximal at the knee of curve, when measured as horizontal width (Fig. 2B). The difference increased in a centripetal manner from the outermost location at BMO-VRW to the knee of curve.

Due to thicker measurements in NAION, BMO-HRW and horizontal/vertical thickness at knee of curve were not

TABLE 1. Baseline Characteristics of the Study Group

	NAION (A)	NTG (B)	Control (C)	*P* Value*	Adjusted *P* Value† (A–B)
Sex, female/male	2/10	8/4	4/8	**0.024**	**0.039**
Age, years	55.2 ± 9.8	61.0 ± 6.6	58.1 ± 7.9	0.907	0.459
MD, dB	−4.91 ± 5.89	−3.42 ± 3.20	−0.97 ± 1.77	0.497	0.717
PSD, dB	7.51 ± 5.56	7.02 ± 4.07	2.09 ± 1.05	**0.008**	1.000
Refractive error, D	−0.98 ± 2.86	−0.91 ± 1.99	−0.43 ± 2.14	0.867	1.000
IOP at examination, mmHg	14.2 ± 2.8	16.2 ± 3.4	14.8 ± 2.1	0.862	0.582
Ovality index	1.05 ± 0.03	1.05 ± 0.03	1.04 ± 0.02	0.979	1.000
Global RNFL thickness, μm	75.1 ± 10.9	77.4 ± 9.1	91.8 ± 12.1	**0.001**	1.000
Sector RNFL thickness, μm	50.2 ± 10.8	61.6 ± 13.2	129.8 ± 15.0	**<0.001**	0.123
Involved hemifields	Superior (11) Inferior (1)	Superior (1) Inferior (11)			

Boldface *P* values indicate statistical significance. MD, mean deviation; PSD, pattern standard deviation; dB, decibel.

* Friedman's test for continuous variables and Pearson χ^2 test for categoric variables.

† Wilcoxon signed-rank test for continuous variables, and Pearson χ^2 test for categorical variables. Adjustment of *P* value with Bonferroni correction for multiple comparisons.

Table 2. Distribution of Local Prelaminar and Neuroretinal Rim Tissue Thicknesses in NAION, NTG, and Controls

Parameter	NAION (A)	NTG (B)	Control (C)	*P* Value*	*P* Value† (A–B)	*P* Value† (A–C)
Disc area, mm^2	2.33 ± 0.33	2.33 ± 0.34	2.38 ± 0.31	0.127	1.000	0.915
BMO width, μm	1635.5 ± 127.6	1687.2 ± 155.5	1688.4 ± 126.9	0.097	0.408	0.150
Central prelaminar tissue thickness, μm	127.4 ± 61.3	81.1 ± 62.3	69.3 ± 25.4	**0.006**	**0.030**	**0.015**
Vertical thickness at the knee of curve, μm	156.9 ± 52.3	141.0 ± 49.9	135.1 ± 26.6	0.558	0.717	0.474
Horizontal thickness at the knee of curve, μm	428.8 ± 94.7	224.7 ± 139.8	384.5 ± 74.5	**0.010**	**0.009**	0.858
BMO-HRW, μm	263.4 ± 83.4	103.8 ± 61.6	295.7 ± 72.3	**<0.001**	**0.006**	0.924
BMO-MRW, μm	136.9 ± 30.1	84.8 ± 45.4	228.5 ± 38.9	**<0.001**	**0.021**	**0.006**
BMO-VRW, μm	166.7 ± 35.4	121.5 ± 53.3	285.7 ± 45.7	**<0.001**	0.084	**0.006**
HV ratio	1.63 ± 0.61	0.83 ± 0.20	1.06 ± 0.31	**<0.001**	**0.006**	**0.030**

Boldface *P* values indicate statistical significance.

* Friedman's test.

† Wilcoxon signed-rank test. Adjustment of *P* value for multiple comparison with Bonferroni correction.

different from those of controls ($P = 0.924$, 0.858, and 0.474). Central prelaminar thickness was even greater in NAION than in controls ($P = 0.005$). Consistently, the HV ratio showed an average value of 1.63 in NAION, significantly exceeding that of controls of around 1.0 ($P = 0.020$). HV ratio of glaucoma was significantly lower than that of NAION ($P = 0.002$).

The reason for this distribution pattern appeared to be the disproportionately thick prelaminar tissue in NAION eyes (Fig. 3A). In glaucoma, tissue thinning was generalized along the course in the NRR (Fig. 3B). The thickness difference compared to that in glaucoma was significant inside the ONH. In eight (66.7%) NAION patients whose sector RNFL was thinner than 50 μm, we noticed a characteristic morphology, resembling the head of a hummingbird (Fig. 3C). The unique shape was formed by joining of the thinned RNFL to the relatively preserved prelaminar tissue thickness in NAION.

Discussion

In the diagnosis of optic neuropathies, the presence of cupping or excavation is an important sign for differentiating between glaucoma and non-glaucomatous conditions. Cupping with rim thinning is a characteristic finding in glaucoma, while it is usually absent in nonglaucomatous optic atrophies.[11,12] Instead, rim pallor was reported to be 94% specific for detection of nonglaucomatous optic atrophy.[13] Development in technology enabled quantitative evaluations, which could prove to be more accurate than a broad characterization according to features such as pallor or cupping. Studies using HRT showed that ONH parameters were significantly different between OAG and NAION.[6,14] The comparative results were based on surface contour evaluations, analysis on cross-section images from OCT followed thereafter. Using an OCT device (Stratus; Carl Zeiss Meditec), increase in cup-to-disc ratio after the development of NAION in 47.8% of eyes when compared to the fellow eyes has been reported.[15] Furthermore, BMO-MRW was suggested as a valid method for evaluation of RNFL thickness,[16–20] as this can provide a direct estimate of the degree of NRR changes. Specifically, a recent promising investigation showed that we might help differentiate between glaucoma and NAION by BMO-MRW measurement.[8]

Nevertheless, despite successful quantified evaluation of the NRR in NAION and glaucoma, the marked difference between pallor and glaucomatous excavation in clinical settings indicates additional contributing factors other than simply magnitude. The reason for selective sparing of rim width decrease in NAION despite a comparable degree of axonal loss compared to glaucoma is not fully elucidated.

Our findings support the view that prelaminar changes in NAION are not a downsized version of those in glaucoma. We investigated how local prelaminar tissue thickness distribution differed between NAION and glaucoma. BMO-VRW measured at a location adjacent to the peripapillary retina, did not differ significantly; however, the thicknesses began to diverge within the ONH. The reason for this might be that BMO-VRW more closely reflects the thickness of axon bundles in the retina. In contrast to a generalized thinning up to the center of the cup in glaucoma, prelaminar tissues inside the cup in NAION maintained significant thickness. The thickness in NAION and in normal eyes was found to be similar, despite the fact that NAION eyes had axonal loss comparable to that of glaucoma.

Several aspects of these findings should be discussed in comparison to previous studies. Fard et al.[7] also studied ONH morphology EDI-OCT in NAION and primary open-angle glaucoma (POAG) patients. They reported profound thinning and posterior displacement of LC in POAG. In addition, there was a marked prelaminar tissue thinning in POAG eyes compared to control and NAION eyes. We did not evaluate depth or thickness of the LC, but our study corroborates theirs in that similar prelaminar tissue thinning was also observed in our study as measured at the center of the LC. Lee et al.[21] reported similar results between NAION and NTG patients in that LC depth was largest in NTG patients, followed by NAION patients, while prelaminar tissue was thinner in NTG patients than in NAION patients. However, NAION patients had a thinner prelaminar tissue relative to normal controls. We consider that the difference was due to a possible complex influence of many components, such as blood vessels, the shape and depth of the LC, and disc size on central prelaminar tissue configuration.

Resch et al.[8] successfully demonstrated the possible usefulness of BMO-MRW in discriminating between glaucoma and NAION. Similar to our findings, NAION patients had similar RNFL thickness values compared with glaucomatous eyes. The lack of difference in BMO-VRW between NAION and glaucoma despite different BMO-MRW in our study group may correspond to the finding. We suggest that the characteristics of axonal loss between NAION and glaucoma might lose their different aspects outside the ONH, especially in locations where the peripapillary RNFL thickness is measured. Clinically, RNFL loss seems indistinguishable in the two conditions on fundus photographs or OCT RNFL thickness measurements. In addition, their result that ONH parameters in NAION eyes were similar to those seen in healthy controls may correspond to our result that within-ONH-parameters including BMO-HRW were statistically similar between NAION and control eyes.

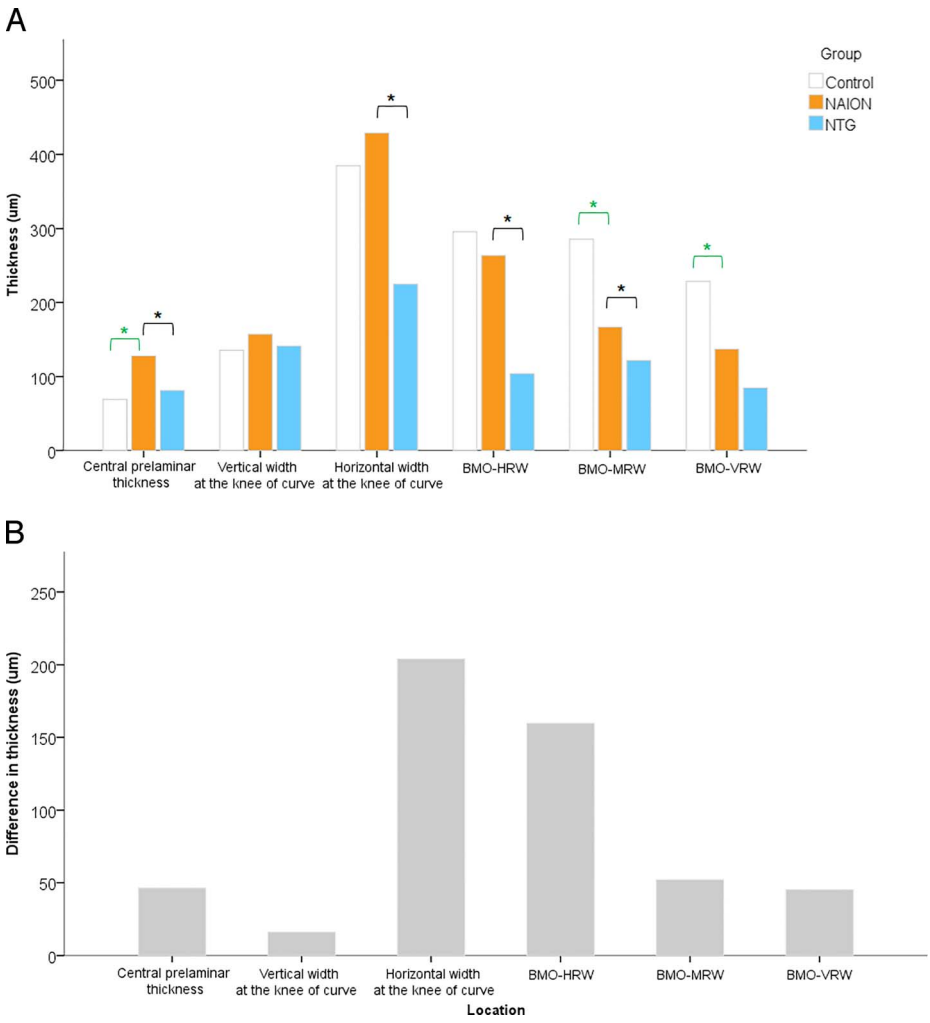

Figure 2. The distribution of local prelaminar and neuroretinal rim thicknesses according to locations in the optic nerve head. (**A**) Thicknesses of prelaminar tissue in a vertical direction above the central LC, knee of curvature, and BMO are shown. The knee of curve shows a point where the curvature has a local maximum around the beginning of the cup wall. Vertical and horizontal widths were measured at the knee of curve, and horizontal, minimal, and vertical rim widths were measured at temporal BMO, all parameters based on BMO plane. *Black asterisks* show a significant difference between NAION and NTG, and *green asterisks* show a significant difference between NAION and controls. (**B**) Difference between NAION and NTG is maximal at the knee of curve in horizontal direction and becomes insignificant at BMO-VRW.

In what manner does the local heterogeneity of distribution lead to disproportionally unchanged rim widths? In other word, what mechanism underlies this unique pattern?

Thick prelaminar tissue remaining exclusively in the horizontal measurement direction seems to be one reason. Because photographic evaluation relies on 2D planimetric view, horizontal width would have a major influence on the cup size measure. This also applies to cup area measurement on HRT. In NAION, significant degree of horizontal cup wall thickness is seen at the level of the cup base when NRR at BMO level is significantly decreased. This may give a false impression that rim thinning is significantly smaller than expected. Nevertheless, the height of the rim does decrease (e.g., as shown by BMO-MRW); this point had been previously addressed by Jonas and Xu,[22] and they mentioned that the optic disc surface flattens in cases of pallor, only to be masked by the pale color.

As for the underlying mechanism, premorbid features in NAION, such as smaller disc size or more voluminous prelaminar tissue, could be possible reasons for a thicker prelaminar tissue after axonal loss compared to that in glaucoma. In NAION, anatomic predisposition exists, with a structurally small, crowded optic disc, or "disc at risk."[23] Saito et al.[5] reported that a smaller disc area and smaller cupping were predisposing risk factors for the development of NAION. Moghimi et al.[24] showed that under similar BMO area and LC depth, the mean prelaminar tissue thickness of the NAION and unaffected fellow eyes was thicker than that of normal subjects. Nevertheless, smaller disc size in NAION has not been yet confirmed; some report smaller discs,[5,22,25] while others show no difference.[7,26,27] In addition, absence of remodeling in LC would also be a significant factor, sparing NAION eyes from deep excavation of LC, apart from prelaminar tissue differences.[28]

The main anatomic components of prelaminar tissue are columns of glial cells, capillaries, and scanty connective tissue that surrounds axon bundles, in contrast to the LC where dense collagenous deposits comprise laminar sheets and glial cells predominate. We could assume that a mechanism may exist that protects or spares these column structures from loss. NAION is believed to be caused by acute, transient ischemic insults, such as hypoperfusion in the short posterior ciliary artery circulation.[29,30] Interestingly, in ischemic optic neuropathy, sparing of glial cells has been documented in histologic

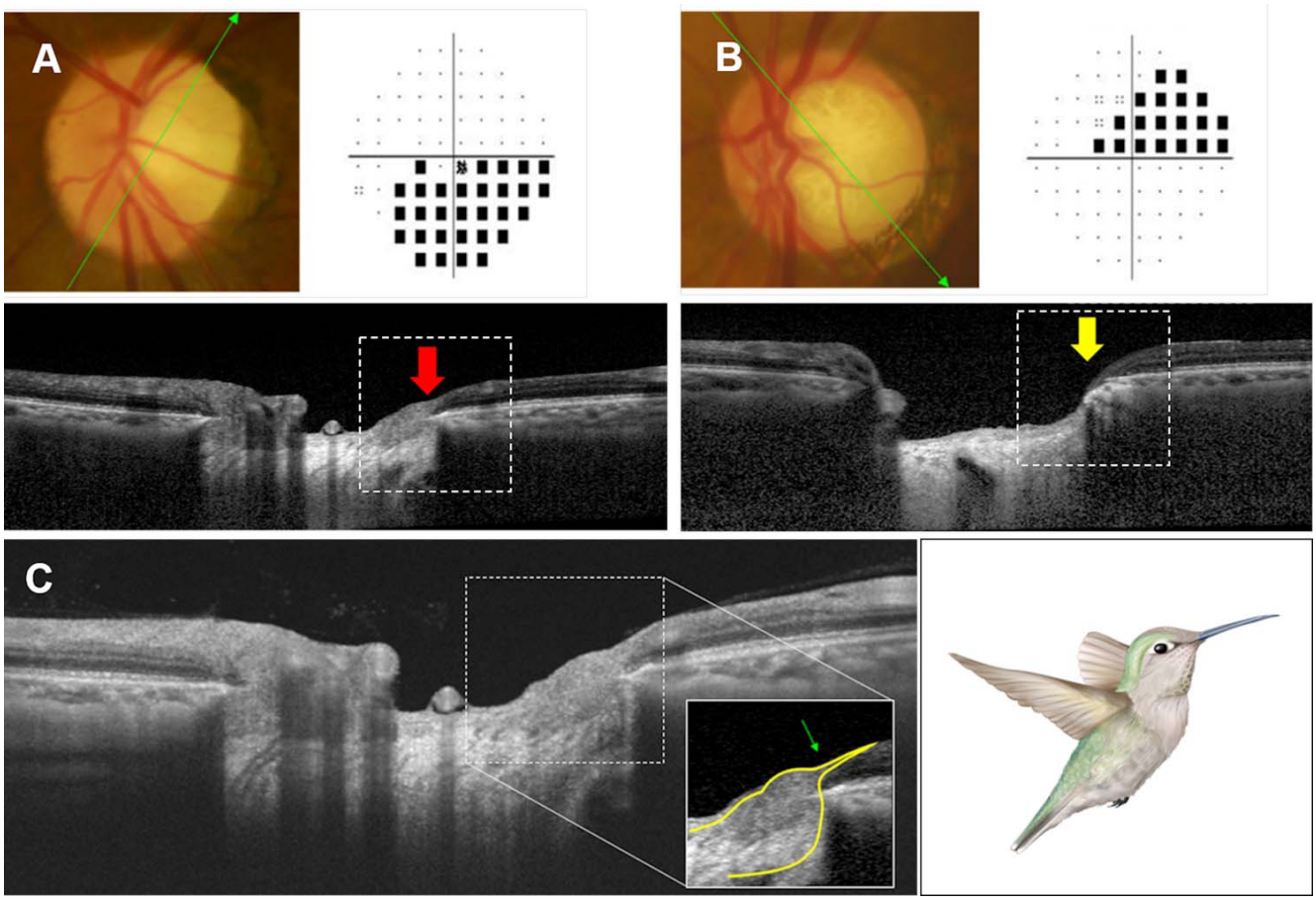

FIGURE 3. OCT images of prelaminar and neuroretinal rim (NRR) area in non-arteritic anterior ischemic optic neuropathy (NAION) and glaucoma. A NAION case with inferior visual field defect (**A**) and an NTG case with superior visual field defect (**B**). (**A**) In NAION, OCT in the direction of pallor shows thinned RNFL up to the outermost margin of the NRR, which would correspond to BMO-VRW. Within ONH, from BMO-MRW and inward, prelaminar tissue is less significantly thinned (*red arrow*), especially compared to that in glaucoma (**B**). Note RNFL thinning in the retinal part is similar, while the horizontal width of the cup wall at the cup base level shows a marked difference between NAION and glaucoma. (**C**) In 8 (66.7%) NAION patients with affected sector RNFL thickness <50 μm, the disproportionate changes in thicknesses resulted in a shape reminiscent of the head of a hummingbird.

studies.[31] Glial cells are thought to be resistant to ischemia and mechanical stress,[32–34] strengthening the likelihood of their survival after ischemic insults, especially those of an acute nature. It would be more beneficial if in vivo imaging could be applied for visualization of glial cells in the future.

The limitations of the present study include the small number of patients. The small study sample size was a result of our strict exclusion criteria and the design of matched analysis. This instead maximized homogeny of patients and provided a more reliable comparison than one without matching. Furthermore, the number was sufficient for statistical analysis. In addition, the findings in this study retain their clarity and importance because all OCT findings were highly consistent and clearly visualized. Nevertheless, it is still possible that marginally significant results, such as BMO-VRW, might show different results with larger number of patients. It is an inevitable fact that the six parameters cannot represent the subtle local curvatures and diversities of the prelaminar tissue. However, there have been no studies on the local distribution of prelaminar tissue so far, and we expect to complement them with further investigations. Nevertheless, our results are sufficient for demonstrating local, within-ONH differences in thickness. Because we ensured that the study excluded patients with ascending optic atrophies, and our sample comprised patients with a descending optic atrophy of acute ischemic pathology, it remains unknown if other optic neuropathies with optic disc pallor would show identical changes. This would also benefit from further investigations. Lastly, OCT imaging has the advantage of being an in vivo technology, but it cannot equal histologic findings. Elucidation of cellular level pathologies are needed in the future.

In conclusion, sparing of prelaminar tissue loss characterized the ONH in NAION against that of NTG with comparable axonal degeneration. Detailed OCT evaluation of NRR changes at multiple locations enabled more detailed anatomic information than global measures. OCT might aid in differential diagnosis based on local patterns of prelaminar tissue thickness. In the future, histopathologic evaluation is warranted to confirm our findings.

Acknowledgments

Disclosure: **E.J. Lee**, None; **J.C. Han**, None; **D.Y. Park**, None; **C. Kee**, None

References

1. Jonas JB, Bergua A, Schmitz-Valckenberg P, Papastathopoulos KI, Budde WM. Ranking of optic disc variables for detection of

glaucomatous optic nerve damage. *Invest Ophthalmol Vis Sci*. 2000;41:1764–1773.

2. Jonas JB, Fernandez MC, Sturmer J. Pattern of glaucomatous neuroretinal rim loss. *Ophthalmology*. 1993;100:63–68.
3. Trobe JD, Glaser JS, Cassady JC. Optic atrophy. Differential diagnosis by fundus observation alone. *Arch Ophthalmol*. 1980;98:1040–1045.
4. Jonas JB, Hayreh SS, Tao Y, Papastathopoulos KI, Rensch F. Optic nerve head change in non-arteritic anterior ischemic optic neuropathy and its influence on visual outcome. *PLoS One*. 2012;7:e37499.
5. Saito H, Tomidokoro A, Tomita G, Araie M, Wakakura M. Optic disc and peripapillary morphology in unilateral nonarteritic anterior ischemic optic neuropathy and age- and refraction-matched normals. *Ophthalmology*. 2008;115:1585–1590.
6. Danesh-Meyer HV, Boland MV, Savino PJ, et al. Optic disc morphology in open-angle glaucoma compared with anterior ischemic optic neuropathies. *Invest Ophthalmol Vis Sci*. 2010;51:2003–2010.
7. Fard MA, Afzali M, Abdi P, et al. Optic nerve head morphology in nonarteritic anterior ischemic optic neuropathy compared to open-angle glaucoma. *Invest Ophthalmol Vis Sci*. 2016;57:4632–4640.
8. Resch H, Mitsch C, Pereira I, et al. Optic nerve head morphology in primary open-angle glaucoma and nonarteritic anterior ischaemic optic neuropathy measured with spectral domain optical coherence tomography. *Acta Ophthalmol*. 2018;96:e1018–e1024.
9. Shoji T, Kuroda H, Suzuki M, et al. Correlation between lamina cribrosa tilt angles, myopia and glaucoma using OCT with a wide bandwidth femtosecond mode-locked laser. *PLoS One*. 2014;9:e116305.
10. Faul F, Erdfelder E, Lang AG, Buchner A. G*Power 3: a flexible statistical power analysis program for the social, behavioral, and biomedical sciences. *Behav Res Methods*. 2007;39:175–191.
11. Hayreh SS. Optic disc changes in glaucoma. *Br J Ophthalmol*. 1972;56:175–185.
12. Jonas JB, Budde WM. Diagnosis and pathogenesis of glaucomatous optic neuropathy: morphological aspects. *Prog Retin Eye Res*. 2000;19:1–40.
13. Trobe JD, Glaser JS, Cassady J, Herschler J, Anderson DR. Nonglaucomatous excavation of the optic disc. *Arch Ophthalmol*. 1980;98:1046–1050.
14. Saito H, Tomidokoro A, Sugimoto E, et al. Optic disc topography and peripapillary retinal nerve fiber layer thickness in nonarteritic ischemic optic neuropathy and open-angle glaucoma. *Ophthalmology*. 2006;113:1340–1344.
15. Contreras I, Rebolleda G, Noval S, Munoz-Negrete FJ. Optic disc evaluation by optical coherence tomography in non-arteritic anterior ischemic optic neuropathy. *Invest Ophthalmol Vis Sci*. 2007;48:4087–4092.
16. Povazay B, Hofer B, Hermann B, et al. Minimum distance mapping using three-dimensional optical coherence tomography for glaucoma diagnosis. *J Biomed Opt*. 2007;12:041204.
17. Chauhan BC, Burgoyne CF. From clinical examination of the optic disc to clinical assessment of the optic nerve head: a paradigm change. *Am J Ophthalmol*. 2013;156:218–227 e212.
18. Danthurebandara VM, Sharpe GP, Hutchison DM, et al. Enhanced structure-function relationship in glaucoma with an anatomically and geometrically accurate neuroretinal rim measurement. *Invest Ophthalmol Vis Sci*. 2014;56:98–105.
19. Chauhan BC, O'Leary N, AlMobarak FA, et al. Enhanced detection of open-angle glaucoma with an anatomically accurate optical coherence tomography-derived neuroretinal rim parameter. *Ophthalmology*. 2013;120:535–543.
20. Pollet-Villard F, Chiquet C, Romanet JP, Noel C, Aptel F. Structure-function relationships with spectral-domain optical coherence tomography retinal nerve fiber layer and optic nerve head measurements. *Invest Ophthalmol Vis Sci*. 2014;55:2953–2962.
21. Lee EJ, Choi YJ, Kim TW, Hwang JM. Comparison of the deep optic nerve head structure between normal-tension glaucoma and nonarteritic anterior ischemic optic neuropathy. *PLoS One*. 2016;11:e0150242.
22. Jonas JB, Xu L. Optic disc morphology in eyes after nonarteritic anterior ischemic optic neuropathy. *Invest Ophthalmol Vis Sci*. 1993;34:2260–2265.
23. Burde RM. Optic disk risk factors for nonarteritic anterior ischemic optic neuropathy. *Am J Ophthalmol*. 1993;116:759–764.
24. Moghimi S, Afzali M, Akbari M, et al. Crowded optic nerve head evaluation with optical coherence tomography in anterior ischemic optic neuropathy. *Eye (Lond)*. 2017;31:1191–1198.
25. Mansour AM, Shoch D, Logani S. Optic disk size in ischemic optic neuropathy. *Am J Ophthalmol*. 1988;106:587–589.
26. Nagia L, Huisingh C, Johnstone J, et al. Peripapillary pachychoroid in nonarteritic anterior ischemic optic neuropathy. *Invest Ophthalmol Vis Sci*. 2016;57:4679–4685.
27. Chan CK, Cheng AC, Leung CK, et al. Quantitative assessment of optic nerve head morphology and retinal nerve fibre layer in non-arteritic anterior ischaemic optic neuropathy with optical coherence tomography and confocal scanning laser ophthalmoscopy. *Br J Ophthalmol*. 2009;93:731–735.
28. Burgoyne C. The morphological difference between glaucoma and other optic neuropathies. *J Neuroophthalmol*. 2015;35:S8–S21.
29. Hayreh SS. Ischemic optic neuropathy. *Prog Retin Eye Res*. 2009;28:34–62.
30. Miller NR, Arnold AC. Current concepts in the diagnosis, pathogenesis and management of nonarteritic anterior ischaemic optic neuropathy. *Eye (Lond)*. 2015;29:65–79.
31. Anderson DR, Davis EB. Retina and optic nerve after posterior ciliary artery occlusion. An experimental study in squirrel monkeys. *Arch Ophthalmol*. 1974;92:422–426.
32. Gurer G, Gursoy-Ozdemir Y, Erdemli E, Can A, Dalkara T. Astrocytes are more resistant to focal cerebral ischemia than neurons and die by a delayed necrosis. *Brain Pathol*. 2009;19:630–641.
33. Anderson DR, Davis EB. Sensitivities of ocular tissues to acute pressure-induced ischemia. *Arch Ophthalmol*. 1975;93:267–274.
34. Hayreh SS, Baines JA. Occlusion of the posterior ciliary artery. 3. Effects on the optic nerve head. *Br J Ophthalmol*. 1972;56:754–764.

Investigative Ophthalmology & Visual Science